

supplementary material for:

Formation of nanocrystalline manganese oxide in flames: oxide phase governed by classical nucleation and size-dependent equilibria

Shruthi Dasappa, Joaquin Camacho

Mechanical Engineering Department, San Diego State University, San Diego, California 92182, USA

Corresponding Author:

Joaquin Camacho

Mechanical Engineering Department

5500 Campanile Dr. E323

San Diego, CA 92182

Phone: 619-594-6076

Fax: 619-594-3599

Email: jcamacho@sdsu.edu

Submitted to *CrystEngComm*

Contents

Table S1 Detailed flame conditions studied

Figure S1 Comparison of measured flame position between MMT doped flames and base flames without doping for B5-B8

Figure S2 XRD patterns after baseline correction for A series deposited materials.

Figure S3 Computed axial temperature profile (OPPDIF) with increasing global strain rate for Flame A.

Figure S4 Saturation ratio-reaction time profiles for $S_0 - S_3$ in the A series flame with saturation ratios calculated with a +/- 100 K temperature-time history.

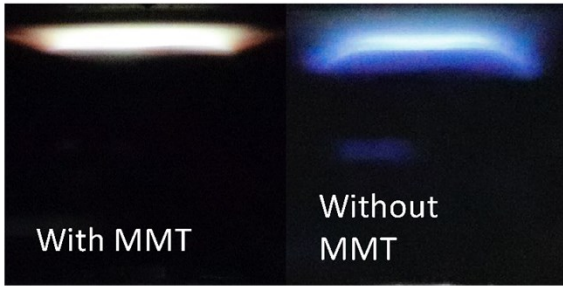
Figure S5 Saturation ratio-reaction time profile for MnO condensation in A flame for no conversion and 99% conversion

Table S.1 Detailed flame conditions studied

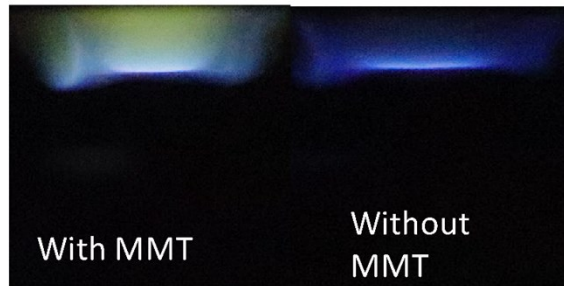
Flame	Φ	$X_{C_2H_4}$	X_{O_2}	X_{Ar}	$T_{f,max}$ (K)	T_{ad} (K)	$t_p(L_{plate})$ (ms)	v_o (cm/s)	Global strain (s^{-1})	MMT (ppm)
A1	0.4	0.063	0.477	0.460	2600	2586	4	335	132	200
A2	0.4	0.063	0.477	0.460	2600	2586	4	335	132	300
A3	0.4	0.063	0.477	0.460	2600	2586	4	335	132	500
B1	0.4	0.056	0.423	0.520	2510	2509	4	301	119	100
B2	0.4	0.063	0.477	0.460	2600	2586	4	335	132	100
B3	0.4	0.056	0.423	0.520	2510	2509	4	301	119	200
B4	0.4	0.063	0.477	0.460	2600	2586	4	335	132	200
B5	0.4	0.045	0.335	0.620	2340	2333	7	252	99	500
B6	0.4	0.051	0.384	0.560	2450	2439	6	290	114	500
B7	0.4	0.056	0.423	0.520	2510	2509	4	301	119	500
B8	0.4	0.063	0.477	0.460	2600	2586	4	335	132	500
C1	0.4	0.063	0.477	0.460	2600	2586	4	335	132	100
C2	0.5	0.056	0.336	0.610	2560	2549	5	299	118	100
C3	0.6	0.055	0.277	0.670	2590	2560	5	305	120	100
C4	0.8	0.060	0.225	0.720	2620	2631	5	316	124	100
D1	1.2	0.054	0.135	0.810	2390	2425	7	267	105	200
D2	1.3	0.064	0.149	0.790	2480	2491	6	279	110	200
D3	1.4	0.067	0.144	0.790	2400	2410	7	269	106	200
D4	1.5	0.074	0.149	0.780	2390	2395	6	279	110	200

Note: Maximum flame temperature, $T_{f,max}$, is based on the computed axial temperature profile from OPPDIF using measured $T(L=0) = 400$ K and $T(L=L_{plate}=2.54 \text{ cm}) = 473$ K as boundary conditions. The adiabatic flame temperature, T_{ad} , is for the unburned mixture at $T = 400$ K. The global strain rate (v_o / L_{plate}) is based on the inlet cold gas velocity, v_o .

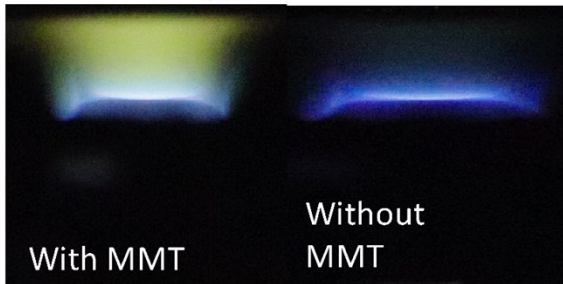
$\Phi = 0.40, T_{f,max} = 2340 \text{ K}, t = 7 \text{ ms}$



$\Phi = 0.40, T_{f,max} = 2450 \text{ K}, t = 6 \text{ ms}$



$\Phi = 0.40, T_{f,max} = 2510 \text{ K}, t = 4 \text{ ms}$



$\Phi = 0.40, T_{f,max} = 2600 \text{ K}, t = 4 \text{ ms}$

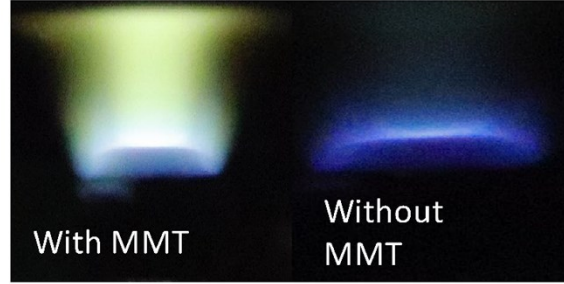


Figure S.1 Comparison of measured flame position between MMT doped flames and base flames without doping for B5-B8.

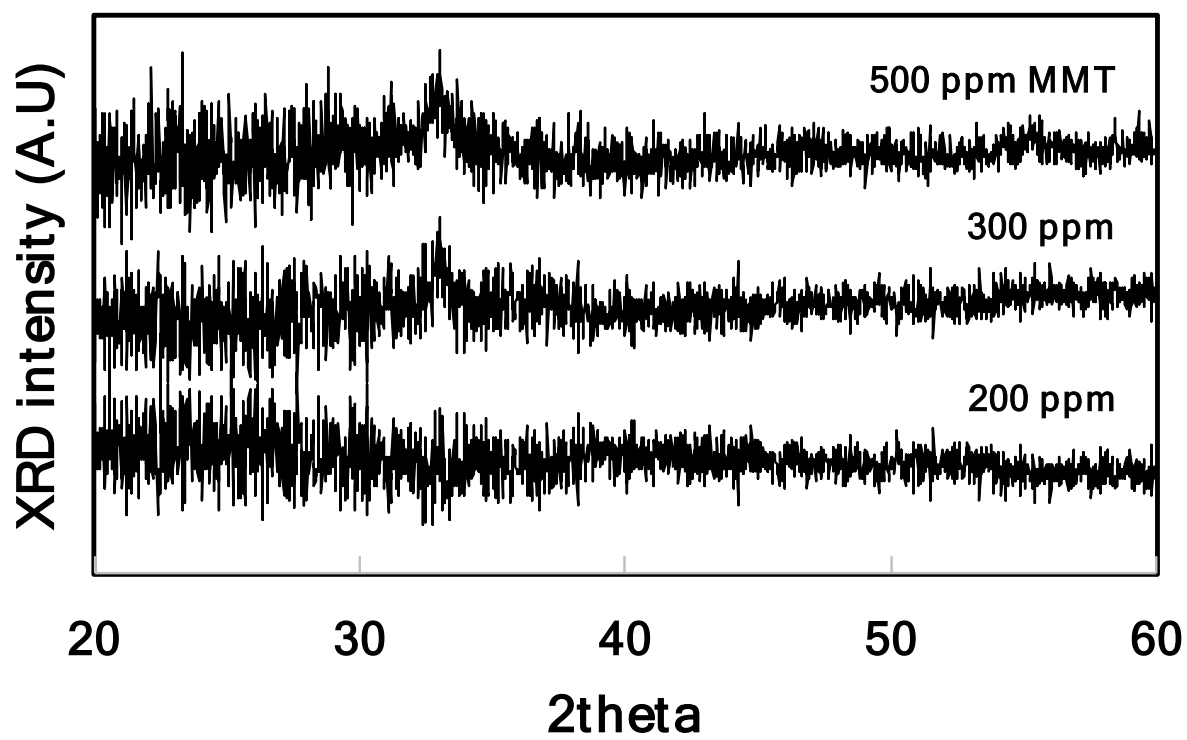


Figure S.2 XRD patterns after baseline correction for A series deposited materials.

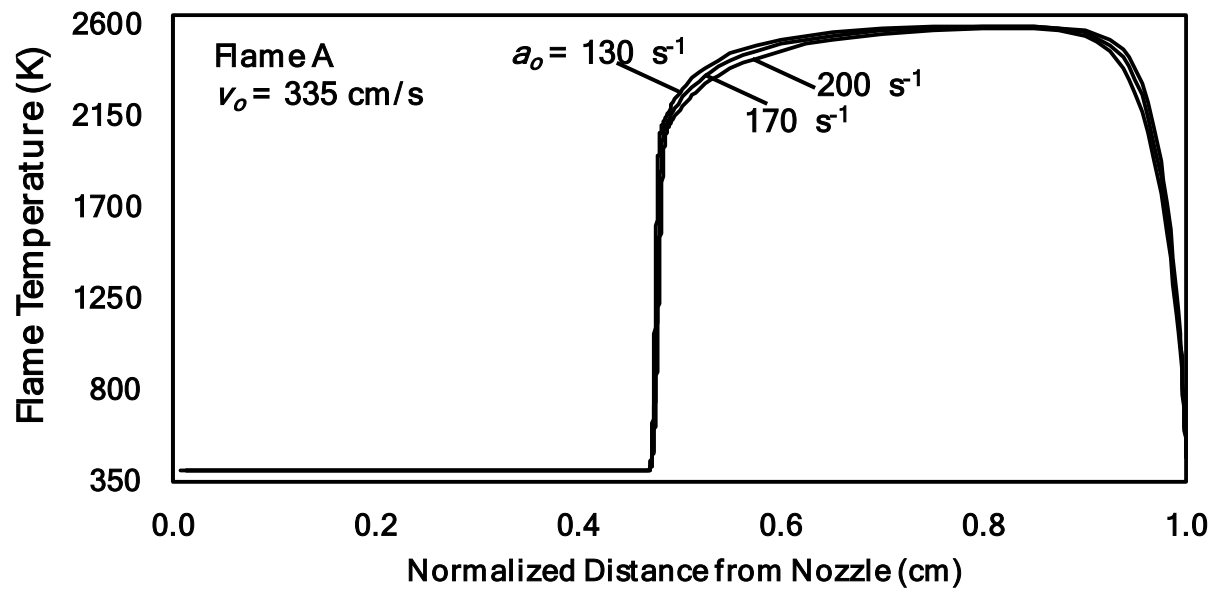


Figure S3 Computed axial temperature profile (OPPDIF) with increasing global strain rate for Flame A.

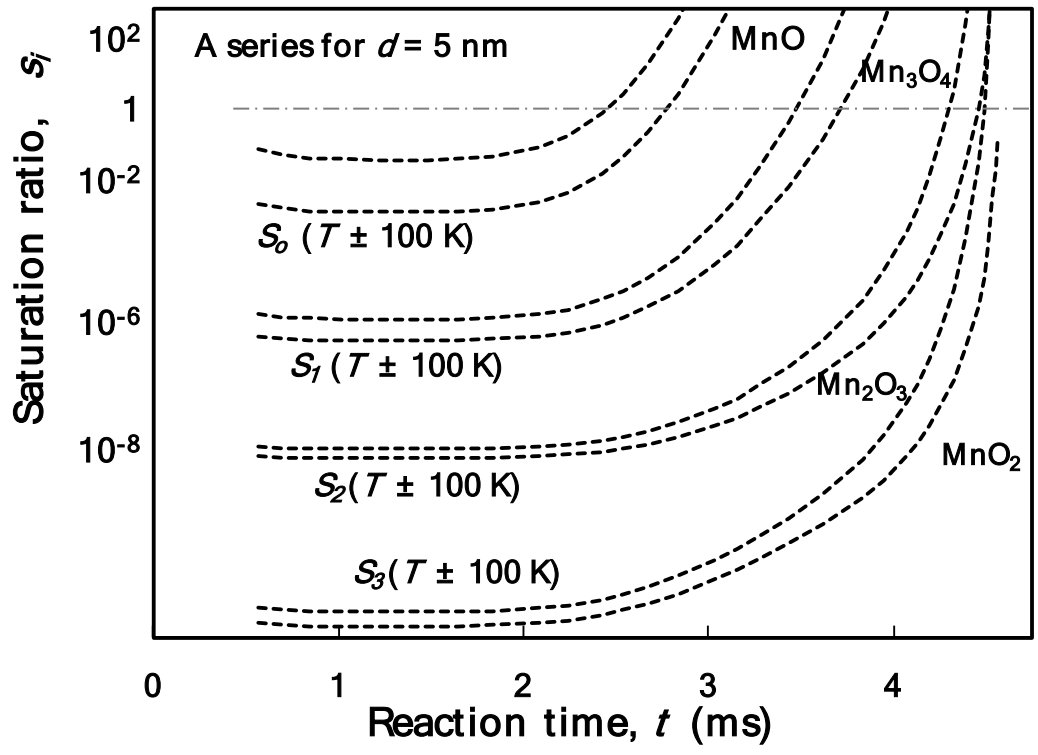


Figure S.4 Saturation ratio-reaction time profiles for $S_0 - S_3$ in the A series flame with saturation ratios calculated with a temperature-time history ± 100 K the base calculation.

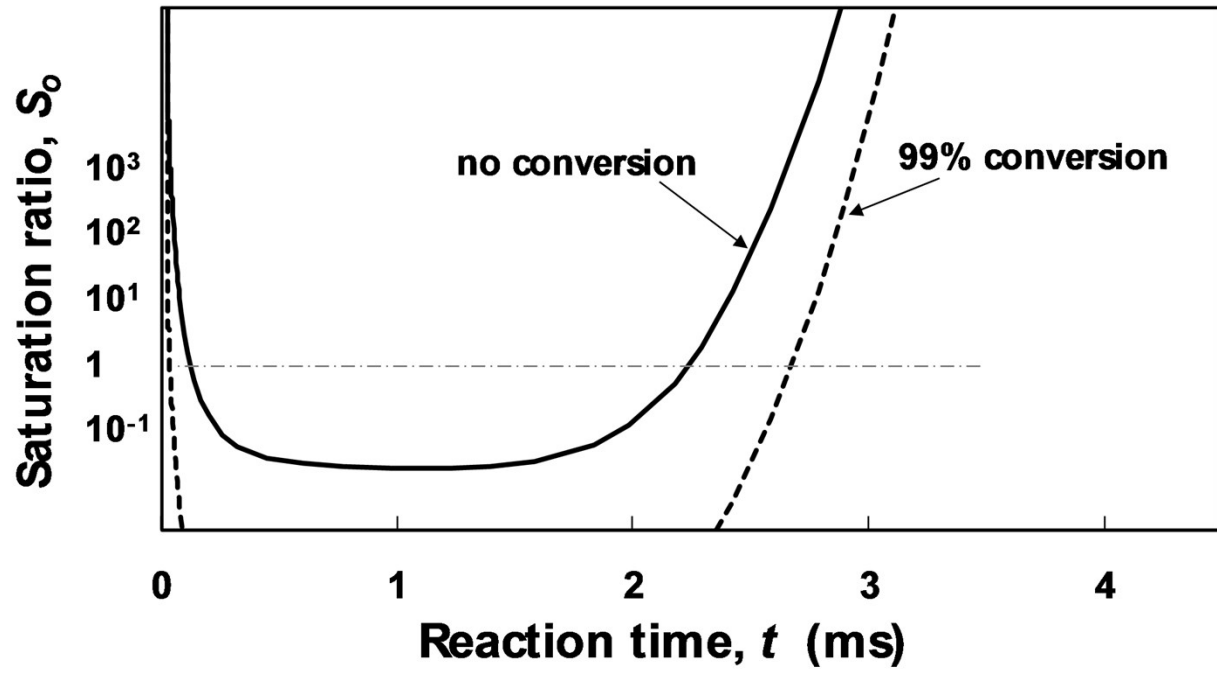


Figure S.5 Saturation ratio-reaction time profile for MnO condensation in A flame for no conversion and 99% conversion